



ELSEVIER

Contents lists available at ScienceDirect

Translational Oncology

journal homepage: www.elsevier.com/locate/tranon

Original Research

Development of near-infrared imaging agents for detection of junction adhesion molecule-A protein

E. Walker^{a,g,*}, S.M. Turaga^{b,c}, X. Wang^a, R. Gopalakrishnan^d, S. Shukla^e, J.P. Basilion^{a,d,g,1}, J.D. Lathia^{b,c,f,g,1}

^a Department of Biomedical Engineering, Case Western Reserve University, Wearn Building, 11100 Euclid Ave., Cleveland, OH 44106-5056, USA

^b Lerner Research Institute, 9500 Euclid Avenue, NC10, Cleveland, OH 44195, USA

^c Department of Biological, Geological, and Environmental Sciences, Cleveland State University, 2121 Euclid Ave., Cleveland, OH 44115, USA

^d Department of Radiology, Case Center for Imaging Research, Case Western Reserve University, 11100 Euclid Ave, Cleveland, OH 44106-7207, USA

^e Department of Urology at the University of Florida College of Medicine, Faculty Clinic, 653 West 8th Street, FC12, Jacksonville, FL 32209, USA

^f Department of Molecular Medicine, Cleveland Clinic Lerner College of Medicine of Case Western Reserve University, 9500 Euclid Avenue, NC10, Cleveland, OH 44195, USA

^g Case Comprehensive Cancer Center, Cleveland, OH 44106, USA



ARTICLE INFO

Keywords:

Molecular imaging
Junctional adhesion molecule-A
Breast cancer
Prostate cancer

ABSTRACT

Introduction: Prostate and breast cancer are the most prevalent primary malignant human tumors globally. Prostatectomy and breast conservative surgery remain the most common definitive treatment option for the >500,000 men and women newly diagnosed with localized prostate and breast cancer each year only in the US. Morphological examination is the mainstay of diagnosis but margin under-sampling of the excised cancer tissue may lead to local recurrence. In spite of the progress of non-invasive optical imaging, there is still a clinical need for targeted optical imaging probes that could rapidly and globally visualize cancerous tissues.

Methods: Elevated expression of junctional adhesion molecule-A (JAM-A) on tumor cells and its multiple pro-tumorigenic activity make the JAM-A a candidate for molecular imaging. Near-infrared imaging probe, which employed anti-JAM-A monoclonal antibody (mAb) phthalocyanine dye IR700 conjugates (JAM-A mAb/IR700), was synthesized and used to identify and visualize heterotopic human prostate and breast tumor mouse xenografts *in vivo*.

Results: The intravenously injected JAM-A mAb/IR700 conjugates enabled the non-invasive detection of prostate and breast cancerous tissue by fluorescence imaging. A single dose of JAM-A mAb/IR700 reduced number of mitotic cancer cells *in vivo*, indicating theranostic ability of this imaging agent. The JAM-A mAb/IR700 conjugates allowed us to image a specific receptor expression in prostate and breast tumors without post-image processing.

Conclusion: This agent demonstrates promise as a method to image the extent of prostate and breast cancer *in vivo* and could assist with real-time visualization of extracapsular extension of cancerous tissue.

Introduction

Breast cancer (BCa) is the most common cancer in women and approximately 1 in 8 US women (12%) will develop invasive BCa over the course of her lifetime. In 2016, an estimated 246,660 new cases of invasive BCa are expected to be diagnosed and approximately 40,450 would die as a result of it [1]. Due to better screening techniques cancers are

caught earlier and 75% of patients are candidates for breast conserving surgery (BCS) to remove the cancer.

Prostate cancer (PCa) remains the most prevalent primary malignant tumor among men in the United States [2]. Radical prostatectomy remains the most common definitive treatment option for the >250,000 men newly diagnosed with localized prostate cancer each year [3], with up to 85% of all prostatectomies in the United States performed robot-

Abbreviations: Breast cancer, BCa; Prostate cancer, PCa; Breast conserving surgery, BCS; Junctional adhesion molecule-A, JAM-A; Target-to-background ratio, TBR; Near infra-red, NIR; Monoclonal antibodies, mAb; Standard deviation, SD.

* Corresponding author at: Department of Biomedical Engineering, Case Western Reserve University, Wearn Building, 11100 Euclid Ave., Cleveland, OH 44106-5056, USA.

E-mail address: yvv@case.edu (E. Walker).

¹ Co-senior authors.

<https://doi.org/10.1016/j.tranon.2020.101007>

Received 21 October 2020; Received in revised form 22 December 2020; Accepted 26 December 2020

1936-5233/© 2021 The Authors. Published by Elsevier Inc. This is an open access article under the CC BY-NC-ND license

(<http://creativecommons.org/licenses/by-nc-nd/4.0/>)

ically [4]. Despite well-developed therapeutic interventions including surgery, radiation, and chemotherapy approximately 35% of patients will develop a prostate-specific antigen recurrence within 10 years after surgery [5,6].

With current screening and public awareness most of BCa and PCa cases detected are estimated to be clinically localized and optimal for surgical treatment. Nevertheless, the status of the microscopic margins of excision of the BCa and PCa specimens is still the most important prognostic and risk factor for local recurrence [7–9]. Unfortunately, despite improving clinical imaging modalities [10,11], the process of achieving negative margins remains retrospective and is determined post hoc by routine pathology exam [12,13]. Indeed, current pathology methods only assess about one tenth of 1% of the entire volume of the removed specimen. So, the ability to visualize small foci of extracapsular extension of both PCa and BCa at the time of surgery may reduce the incidence of positive surgical margins while reducing damage to critical adjacent structures [14]. Targeted optical imaging probes, as imaging tools to visualize cancerous tissue, might be a solution.

Fluorescence imaging is a developing, highly beneficial, and promising approach for assessment of tumor boundaries during surgical procedures that holds many advantages, where among others are a high sensitivity, a real-time visualization, and an ability to assess the entire surgical margins [15,16]. Apart from the relatively low cost of the fluorescent contrast agent, it is considered to be safe for the patient and for the medical team [17]. Several fluorescence probes for detecting the activity of proteases upregulated in BCa cells have been developed to visualize tumors rapidly and sensitively [18–21]. Tumor targeting fluorescent probes, including anti-VEGF Bevacizumab-800CW [22,23] and anti-integrin $\alpha V\beta_3$ rGDY-PEG-Cy5.5-C dots [24], are in clinical trials for fluorescence image guided surgery of BCa and better control of local recurrences. Among many discovered proteins that PCa tissue is expressed, a few were well-characterized and then nominated as specific biomarkers. Agents such as fluorescence-labeled hepsin- and matriptase-targeted peptide and antibody [25–27] have been developed and applied for fluorescence imaging of PCa. Recently, prostate-specific membrane antigen (PSMA) that is highly expressed in PCa was "brought to light" of the fluorescent imaging realm. Levels of PSMA expression might correlate with the stage of PCa disease and Gleason score [28] that made it a promising target for both imaging [29–31] and treatment of prostate cancer [32,33].

Junctional adhesion molecule-A (JAM-A) was discovered 20 years ago, but it was recently described to have a prognostic role in cancer development [34,35]. In addition, JAM-A expression has been demonstrated to be necessary and sufficient for self-renewal and tumor growth, indicating a cell-intrinsic role for JAM-A in biology of malignant tissue [36], making JAM-A a potential new therapeutic target. JAM-A has never been used as a target molecule for any molecular imaging modalities mainly because of its widely expression by many tissues in humans that might potentially lead to a low target-to-background ratio (TBR). We hypothesized that anti-JAM-A monoclonal antibody (mAb) labeled with near infra-red (NIR) IR700 dye (JAM-A mAb/IR700), could be used as an imaging agent to detect tumors *in vivo*. Herein, we describe our initial experience with JAM-A mAb/IR700 conjugates testing this agent in human prostate and breast cancer xenografts in mice. We found that a single dose of our construct demonstrates a sufficient TBR to discriminate tumors and significantly reduces number of mitotic cancer cells *in vivo*, that may indicate a theranostic potential of this construct.

Material and methods

Compliance of ethical standards

All experimental procedures were approved by the Case Western Reserve University Institutional Animal Care and Use Committee (protocol number: 2015-0033).

Reagents

Both mouse blocking JAM-A monoclonal antibodies (mAb) (IgG₁, clone J10.4; sc-53623) and non-specific (normal) mouse IgG Ab (sc-2025) were purchased from Santa Cruz Biotechnology, Inc. (Dallas, Texas, USA). All other chemicals (Sigma-Aldrich Inc.) were of reagent grade.

Synthesis of IR700-conjugated JAM-A mAb and control normal mouse IgG

Before conjugation of dye with mAbs, the azide preservative was removed from the mAbs by buffer exchange for 1X PBS using Zeba spin desalting 2-mL columns (Thermo Scientific, Rockford, IL). Conjugation of dyes with Abs was performed according to IRDye 700DX Low MW Protein Labeling Kit protocol (Li-Cor Bioscience, Lincoln, NE). Briefly, JAM-A mAb or normal IgG (Norm Ab) – both 0.2-mg/mL – were incubated with IR700 NHS ester (5.0-mg/mL) in 0.1 mol/L K₂HPO₄ (pH=8.5) at room temperature for 2-h followed by purification with Zeba spin desalting 2-mL columns at 1000 g for 2-min. The protein concentration was determined by measuring the absorption at 280-nm with Tecan Infinity 200 reader (Tecan Group Ltd., Männedorf, Switzerland). The concentration of IR700 was assessed by absorption at 689-nm to confirm the number of fluorophore molecules conjugated to each IgG molecule.

Radiolabeling of antibodies

As a quality control of the JAM-A mAb/IR700, the levels of immune-binding of intact JAM-A mAb and JAM-A mAb/IR700 conjugates to alive PC3pip cells *in vitro* were assessed. First, JAM-A mAb and JAM-A mAb/IR700 conjugates were labeled with ¹²⁵I Na using a direct protein iodination. Briefly, aliquots of 250- μ Ci ¹²⁵I Na (PerkinElmer, Akron, OH) in Tris-Iodination Buffer were activated in the Pierce Pre-Coated Iodination Tubes (Thermo Scientific, Rockford, IL) followed by mixing with 40- μ g of JAM-A mAbs or IR700 conjugates per tube. After incubation with Scavenging Buffer, mixes were purified with Zeba spin desalting columns at 1000 g for 2-min and elution fractions were collected. Next, for immune-binding assay, the purified radiolabeled JAM-A mAbs or IR700 conjugates were mixed with alive culture of PC3pip cells for 1-h at 4 °C followed by washing and radioactive scan of the collected pellets (Bioscan AR 2000, Bioscan Inc., Washington, DC). PC3pip cells that were blocked by an excess of JAM-A mAb prior these procedures were used as internal controls.

Cell culture

Human PCa retro-virally transformed prostate specific membrane antigen-positive PC3pip cells were obtained from Dr. Michel Sadelain in 2000 (Laboratory of Gene Transfer and Gene Expression, Gene Transfer and Somatic Cell Engineering Facility, Memorial-Sloan Kettering Cancer Center, New York, NY). The cells were last checked by Western blot analysis in 2019; no genetic authentication was performed. Human triple negative mammary carcinoma cell line MDA-MB-231 was obtained from the American Type Culture Collection. All cells were maintained in RPMI-1640 medium (Thermo Scientific, Rockford, IL) with 2 mmol/L L-glutamine and 10% FBS at 37 °C and 5% CO₂ under a humidified atmosphere.

Proliferation assay

Cell proliferation experiments were conducted by plating PC3pip or MDA-MB-231 cells at a density of 1000 cells/well in a 96-well plate in triplicate. Cell number was measured every other day in presence of different concentrations (1-, 5-, and 10- μ g/mL) of Norm Ab or blocking JAM-A mAb in comparison and then normalized to the initial reading at day zero using the CellTiter-Glo assay kit (Promega, Madison, WI).

Western blotting

MDA-MB-231 and PC3pip cells were cultured in 10-cm petri dishes (4×10^6 /dish). Cells were treated with anti-JAM-A mAb or normal IgG for 24-h before lysate preparation. Aliquots of whole cell lysates (25- μ g) were separated on 12% SDS-PAGE and electro-blotted onto nitrocellulose membranes. The membranes were then immunoblotted with antibodies against JAM-A. The membranes were incubated with appropriate peroxidase-labeled secondary antibodies (Dako, Santa Clara, CA), and bands were visualized using enhanced chemiluminescence (GE Healthcare, Buckinghamshire, UK).

Animal and tumor models

All animal procedures were performed according to Institutional Animal Care and Use Committee (IACUC) approved protocols. Animals were fed on a special rodent diet (Harlan Laboratories, Inc.) to reduce autofluorescence. For flank tumor xenografts, 6- to 8-week-old athymic nude mice were implanted subcutaneously with 2×10^6 of MDA-MB-231 or PC3pip cells in 100- μ L Matrigel at the right upper chest (females) or right dorsum flank (males), respectively. Animals were observed every other day until tumors reached at about 150-mm³ in volume.

In vivo fluorescent imaging

Imaging was performed with the aid of the Maestro In Vivo Imaging System (PerkinElmer, Waltham, MA) with each mouse receiving 20- μ g of JAM-A mAb/IR700. For a probe competition, *in vivo* assay, JAM-A mAb/IR700 conjugates (20- μ g) and JAM-A mAb (40- μ g) were mixed immediately before *i.v.* injections. Norm Ab/IR700 conjugates (20- μ g) or IR700 alone (5.0-mg/mL) were used as controls. All compounds were mixed with sterile 1X PBS followed by tail vein injection. Imaging was performed at different time points using deep-red filter set. During imaging, the temperature of imaging bed was kept at 37 °C. Mice received inhalation of isoflurane through a nose cone attached to the imaging bed. Mice were imaged over 2-day post-injection, after which, the mice were sacrificed and tissues such as liver, kidneys, spleen, heart, lung, seminal vesicles along with prostate gland, and tumor xenografts were harvested for *ex vivo* imaging. Quantification of fluorescent signals was obtained by calibration of IR700 using the 780-nm channel.

Fluorescent microscopy

PC3pip and MDA-MB-231 cells were plated on coverslips at about 70% confluency. After incubating overnight to promote adherence, cells were treated with JAM-A mAb/IR700 (final: 12.5- μ g/mL). After incubation for 3-h cells were washed 3 times with PBS, fixed with 4% para-formaldehyde, counterstained with 4',6-diamidino-2-phenylindole (DAPI), mounted with Fluor-Mount aqueous mounting solution, sealed with nail polish, and observed using Leica DM4000B fluorescence microscopy (Leica Microsystem Inc.). Blocking experiments were performed by co-incubation of PC3pip and MDA-MB-231 cells with blocking mix of recombinant human JAM-A Fc chimera protein (R&D Systems, Minneapolis, MN) and JAM-A mAb/IR700 for 1-h (finals: JAM-A mAb/IR700 (12.5- μ g/mL) and JAM-A protein (50- μ g/mL)) at room temperature in the dark.

Immunofluorescent analysis of tumor xenograft samples

Tumors were extracted 48-h after a single *i.v.* injection of JAM-A mAb/IR700 conjugates or controls, snap-frozen in optimum cutting temperature compound, and kept at -80 °C followed by 10- μ m thick cryosectioning at -25 °C (Leica CM3050S, Leica Biosystems). For immune-histochemical analysis, the slides were warmed to room temperature, fixed with 10% buffered formalin, and blocked in blocking

buffer (5% normal goat serum/0.3% Triton X-100 in 1X PBS) for 1-h at room temperature and incubated in primary mAb overnight at 4 °C followed by triple washing in 1X PBS. The tumor expression of phosphorylated-histone H3 (Ser10) was evaluated by rabbit anti-human histone H3 mAb (Cell Signaling) at a 1:200 dilution. After washing, the slides were treated with the secondary ready-to-use antibody (goat anti-rabbit polyclonal antibody labeled by Alexa Fluor-594, Invitrogen, Inc.) for 20-min at room temperature followed by triple washing with 1X PBS for 5-min. Tissue nuclei were contrasted with Fluoro-Gel-II (Electron Microscopy Sciences, Hatfield, PA). If needed, adjacent slides we stained with hematoxylin and eosin by standard procedures.

Statistical analysis

All data are expressed as mean \pm standard deviation (SD). The values are measured values between the groups was performed by one-way analysis of variance (ANOVA) with 95% confidence limits for multiplex analysis, by Mann-Whitney *U*-test, or by Student's *t*-test. The *p* values less than 0.05 was considered as significant for these studies.

Results

In vitro characterization of JAM-A mAb and JAM-A mAb/IR700 conjugates

To assess the utility of JAM-A mAb directed against human JAM-A protein, we evaluated the levels of JAM-A expression in PC3pip and MDA-MB-231 cancer cell lines. When compared to untreated controls, presence of JAM-A mAb reduced levels of JAM-A expression (see Supplementary Fig. S1A) indicating that expression of JAM-A protein in cancer cells may be blocked specifically.

Conjugation of JAM-A mAb or Norm Ab to IR700 resulted in two IR700 molecules conjugated to each mAb or IgG molecule. *In vitro* immunoreactivity of JAM-A mAb/IR700 were analyzed with a binding assay using ¹²⁵I-labeled JAM-A mAb IR700 conjugates along with ¹²⁵I-labeled JAM-A mAb and revealed that $83.27 \pm 4.43\%$ of binding was achieved with JAM-A mAb conjugate. The specificity of binding was confirmed by blocking with excess of native unconjugated JAM-A mAb (less than 5%) (see Supplementary Fig. S1B).

To confirm expression of JAM-A and evaluate the possible impact of disrupting JAM-A on cell growth of PC3pip and MDA-MB-231 cancer cell lines, we utilized the same anti-JAM-A mAb to block the dimerization of JAM-A [36]. Both cancer cell lines treated with the JAM-A mAb at previously reported concentrations of 1- and 10- μ g/mL [36,37] showed significant reduction in growth over a 3-day time course that was both specific and dose-dependent (see Supplementary Fig. S2). This short time course did reveal a significant reduction in PC3pip cell line growth at the 1-, 5-, and 10- μ g/mL antibody concentration (see Supplementary Fig. S2A) as compared with control Norm Ab. A significant reduction in MDA-MB-231 cell line growth was found at the 5- and 10- μ g/mL but not at the 1- μ g/mL JAM-A mAb concentration (see Supplementary Fig. S2B).

To examine the uptake of JAM-A-targeted conjugates, *in vitro* cellular uptake of JAM-A mAb/IR700 in PC3pip and MDA-MB-231 cells were performed and visualized by fluorescent microscopy. No detectable amount of fluorescence uptake was observed in either PC3pip or MDA-MB-231 cells in presence of controls. Indeed, when JAM-A mAb/IR700 was pre-incubated with an excess amount of JAM-A protein (see Supplementary Fig. S2C and D), no fluorescent signal was observed, confirming that cellular uptake of fluorescence was attributed to the specific binding of JAM-A mAb/IR700 conjugates to JAM-A in the cells. Additionally, the presence of Norm Ab/IR700 conjugates also did not visualize both PC3pip and MDA-MB-231 cells. When cells were incubated with JAM-A mAb/IR700, the IR700 fluorescence was detected mainly on the cell surface of MDA-MB-231 cells (see Supplementary Fig. S2D). Whereas the fluorescence was also detected inside the PC3pip cells, indicating

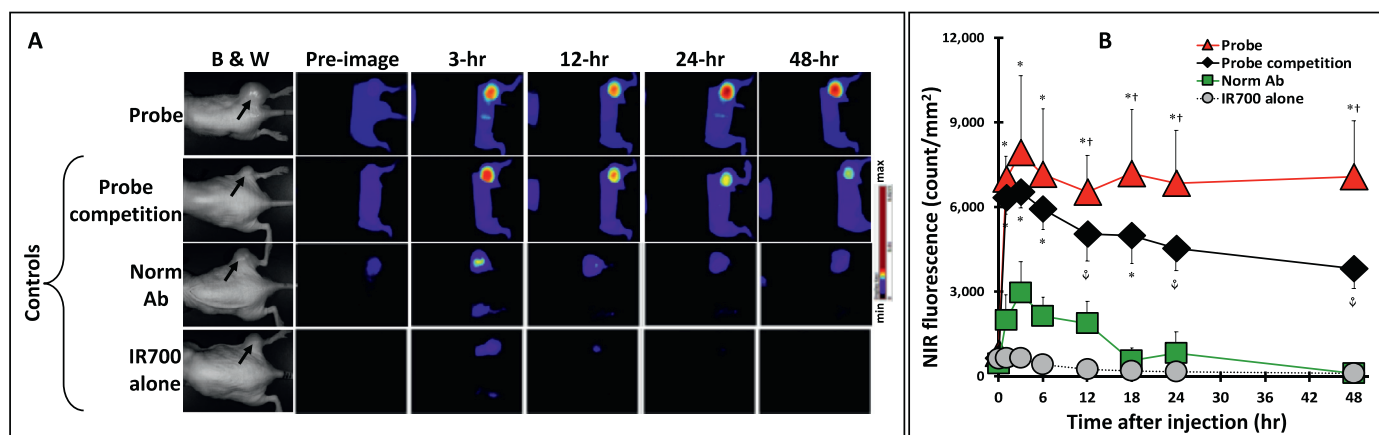


Fig. 1. *In vivo* fluorescence imaging of PC3pip tumor xenografts.

(A) *In vivo* IR700 fluorescence real-time imaging of right flank PC3pip human prostate tumor xenografts in mice after tail vein injection of JAM-A mAb/IR700 (Probe). Controls: 1) mix of JAM-A mAb and JAM-A mAb/IR700 conjugates (2-to-1 ratio, respectively) – Probe competition; 2) non-specific mouse IgG/IR700 conjugates – Norm mAb, and 3) IR700 alone. Black arrows – flank tumors. Pseudo-color images of IR700 fluorescence are presented in the same scale. Back is shielded by a black tape. (B) Quantitative analysis of IR700 intensities in tumors. The IR700 fluorescence intensities were significantly higher in PC3pip tumor xenografts labeled with probe as compared with controls. After pre-image (before *i.v.* injection), images were taken at 1-, 3-, 6-, 12-, 18-, 24-, and 48-h time points. Each time-point indicates an average of IR700 fluorescence per mm² of tumor xenograft. Vertical bars – SD. Data were normalized to the levels of IR700 fluorescence of pre-images, $n = 5$ per each group; * – $p < 0.005$ to Norm Ab & IR700 alone, † – $p < 0.05$ to Probe competition, ‡ – $p < 0.05$ to Norm Ab & IR700 alone (Mann-Whitney-*U* test).

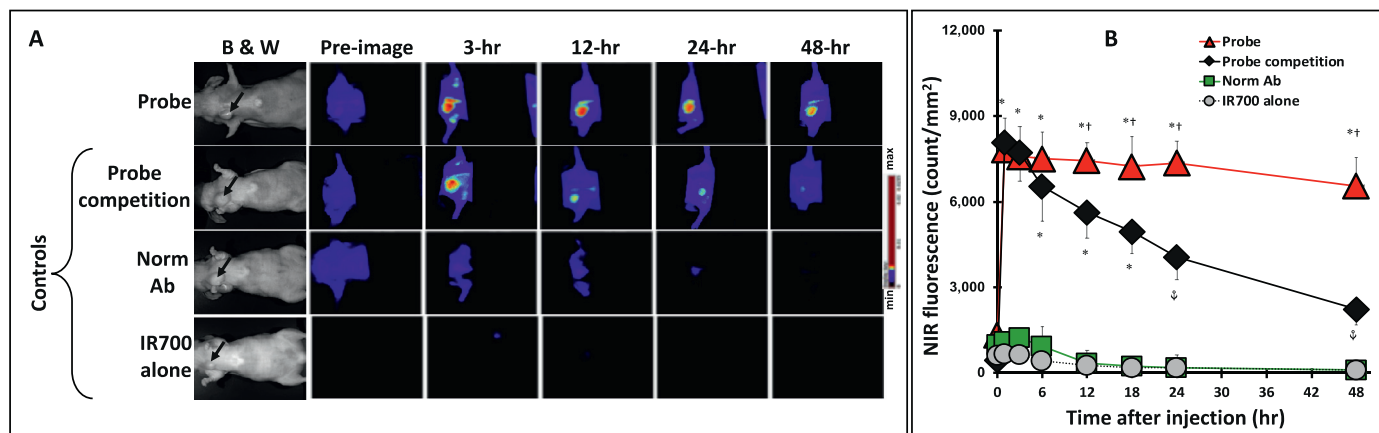


Fig. 2. *In vivo* fluorescence imaging of MDA-MB-231 tumor xenografts.

(A) *In vivo* IR700 fluorescence real-time imaging of left chest MDA-MB-231 human breast tumor xenografts in mice after tail vein injection of JAM-A mAb/IR700 (Probe). Controls: 1) mix of JAM-A mAb and JAM-A mAb/IR700 conjugates (2-to-1 ratio, respectively) – Probe competition; 2) non-specific mouse IgG/IR700 conjugates – Norm mAb, and 3) IR700 alone. Black arrows – chest tumors. Pseudo-color images of IR700 fluorescence are presented in the same scale. Abdomen is shielded by a black tape. (B) Quantitative analysis of IR700 intensities in tumors. The IR700 fluorescence intensities were significantly higher in PC3pip tumor xenografts labeled with probe as compared with controls. After pre-image (before *i.v.* injection), images were taken at 1-, 3-, 6-, 12-, 18-, 24-, and 48-h time points. Each time-point indicates an average of IR700 fluorescence per mm² of tumor xenograft. Vertical bars – SD. Data were normalized to the levels of IR700 fluorescence of pre-images, $n = 5$ per each group, * – $p < 0.005$ to Norm Ab & IR700 alone, † – $p < 0.05$ to Probe competition, ‡ – $p < 0.05$ to Norm Ab & IR700 alone (Mann-Whitney-*U* test).

possible gradual internalization [38] (see Supplementary Fig. S2C) and accumulation in the perinuclear position of the PC3pip cells, concurring with our previous results with IR700 conjugates [39]. Taken together, these data suggest that JAM-A mAb can specifically bind and attenuate growth of PC3pip and MDA-MB-231 cells. Once conjugated with IR700 dye, JAM-A mAb can also specifically visualize both cancer cell lines *in vitro*.

In vivo imaging

Animals bearing PC3pip or MDA-MB-231 tumors were used to demonstrate noninvasive imaging and examine the bio-distribution of IR700 conjugates *in vivo*. As shown in Figs. 1 and 2, strong uptake of JAM-A mAb/IR700 conjugates (Probe) was observed in both PC3pip and MDA-MB-231 tumor xenografts. The levels of fluorescence intensity of JAM-A mAb/IR700 in prostate and breast tumors increased rapidly

and did not decline in time, remaining detectable *in vivo* throughout the study.

To confirm that binding of JAM-A mAb/IR700 to JAM-A in the cancerous tissue was specific, the *in vivo* imaging with controls was performed. First, we found that *i.v.* injection of a mix of JAM-A mAb and JAM-A mAb/IR700 conjugates (Probe competition) led to 1.5–2-fold lower IR700 fluorescence in prostate and breast tumors as compared with JAM-A mAb/IR700 conjugates alone 18-h after injection. Second, the levels of IR700 fluorescence in tumor xenografts were also significantly lower in mice treated with Norm Ab/IR700 conjugates or IR700 alone that may indicate its lower accumulation in cancerous tissue as compared with tested JAM-A mAb/IR700 probe (see Figs. 1B and 2B).

High fluorescence was observed in the middle back of the animals bearing PC3pip tumor xenografts at early time points (see Supplementary Fig. S3A), that was gradually reduced with time; this is likely due to nonspecific accumulation of JAM-A mAb/IR700 in the kidneys.

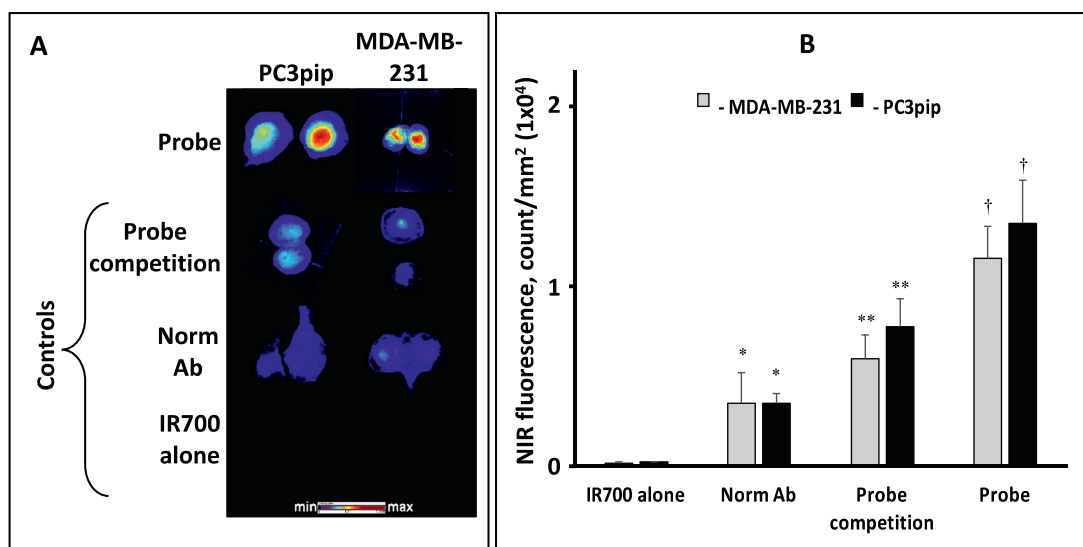


Fig. 3. *Ex vivo* fluorescent imaging of mouse tumor xenografts.

(A) Imaging of tumor xenografts at 48-h post-injection of JAM-A mAb/IR700 and controls. Each xenograft was cut into 2 halves to image internal sides of the tumors. The fluorescence was significantly higher in tumors of animals which were treated with JAM-A mAb/IR700 (*Probe*). Controls: 1) mix of JAM-A mAb and JAM-A mAb/IR700 conjugates (2-to-1 ratio, respectively) – *Probe competition*; 2) non-specific mouse IgG/IR700 conjugates – *Norm mAb*, and 3) *IR700 alone*. Pseudo-color images of IR700 fluorescence are presented in the same scale. (B) Quantitative analysis of IR700 fluorescent intensities in tumor xenografts. Values represent mean of IR700 fluorescence per mm² of internal surfaces of the tumor xenografts. The fluorescence of PC3pip and MDA-MB-231 xenografts was analyzed separately. Vertical bars – SD; n = 5 per each group, † – $p < 0.001$ to all controls; ** – $p < 0.02$ to Norm Ab and IR700 alone; * – $p < 0.05$ to IR700 alone (Mann-Whitney-U test).

Strong fluorescence was also detected in the middle abdominal area of the animals bearing MDA-MB-231 tumor xenografts at the chest at early time points (see Supplementary Fig. S4A), that also gradually reduced with time; this is likely due to nonspecific accumulation of JAM-A mAb/IR700 in the liver, indicating hepatobiliary clearance of this agent, which is typical of antibody clearance [40].

In contrast to IR700 dye alone that was fluorescently silent in mouse bodies, analysis of the levels of fluorescent signals from kidney and liver areas revealed that JAM-A mAb/IR700 (*Probe*), non-specific IgG/IR700 conjugates (*Norm Ab/IR700*), and specific but partially blocked JAM-A mAb/IR700 conjugates (*Probe competition*) induced the same levels of fluorescence from both kidneys and liver (see Supplementary Figs. S3B and S4B). It worth to note that the liver/kidney zones of the mouse bodies were shielded during imaging of the tumor xenografts in Figs. 1 and 2. Although this approach cannot be used in live-image guided surgery, our experience indicates that it might be an issue for small animal models (rodents) rather than for large animal models (dogs). Indeed, a significant distance between Bca/Pca orthotopic tumor xenografts and liver or kidneys along with a necessity to use a light source that can initiate fluorescence at a short distance to a supposed cancer zone (-s) may eliminate a necessity to shield normal tissue/organs during image guided surgery.

Altogether, it may indicate that strong fluorescent signal from these organs is related to ability of IgG to be accumulated non-specifically and transiently in the mesenchymal tissue of these organs rather than to a strong and specific binding of JAM-A Ab/IR700 to target protein [40].

Ex vivo imaging

Mice were euthanized 48-h after injection of JAM-A mAb/IR700 and mouse organs along with PC3pip and MDA-MB-231 tumor xenografts were taken for *ex vivo* imaging. Fig. 3 shows IR700 fluorescence in excised tumors. In these experiments, each xenograft was cut into two halves and the levels of fluorescence from the tumor cores were compared. As Fig. 3A shows, although not always equal but strong IR700 fluorescence was observed at the inner surfaces of tumor xenografts only

in animals which were treated with JAM-A mAb/IR700 conjugates. That levels of IR700 fluorescence were significantly higher than those from the inner cores of tumors in animals which were treated with controls (see Fig. 3B). Although kidney and liver produced higher levels of IR700 fluorescence *ex vivo* (see Supplementary Fig. S5A), statistical analysis revealed that only fluorescence from prostate and breast tumors was both specific and strong as compared with all controls (see Supplementary Fig. S5B).

Ex vivo imaging of frozen tumor tissue

To confirm or rule out a specific accumulation of JAM-A mAb/IR700 conjugates in prostate and breast tumors making them visible *in vivo*, we assessed the levels of IR700 fluorescence in excised tumor xenografts microscopically (see Fig. 4). Fluorescence microscopy of the tumor tissue revealed that cancer tissue of animals that were treated with JAM-A mAb/IR700 produced significantly higher levels of IR700 fluorescent signals (see Fig. 4C and D), indicating specific binding of the studied conjugates to the JAM-A expressing cancer cells *in vivo*. There was no detectable difference of the levels of IR700 fluorescence in prostate and breast tumors in animals that were treated with JAM-A mAb/IR700.

Mitotic activity in tumor xenografts

In our *in vitro* experiments, JAM-A mAb abrogated cell proliferation for both prostate and breast cancer cell lines in a dose-depend manner (see Supplementary Fig. S2A and S2B). Further, we conducted immunohistochemistry study of the levels of mitotic cells in the prostate and breast cancerous tissue to determine whether this blocking ability of JAM-A mAb was preserved *in vivo*. Using a phosphorylated Ser10 of histone H3 that is tightly correlated with chromosome condensation [41] as a marker of the mitosis, we demonstrated that a single dose of JAM-A mAb/IR700 agent decreases number of mitotic cells in cancer tissue (see Fig. 5A). Statistical analysis revealed that absolute number of mitotic cells were similar in cancerous tissue of animals that were treated with controls. However, the levels of H3⁺ mitotic cells were 1.5-fold lower

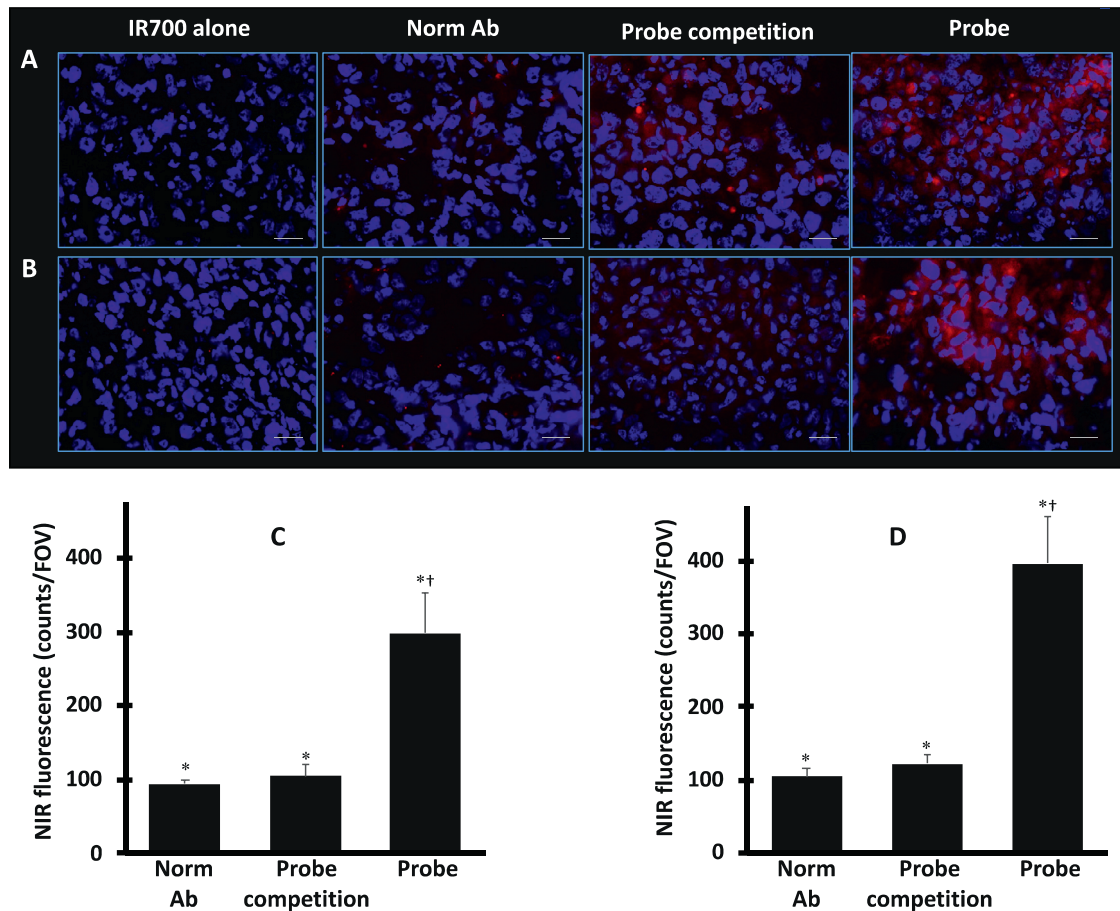


Fig. 4. Accumulation of JAM-A mAb/IR700 in tissue of mouse tumor xenografts. (A) Prostate PC3pip tumor xenograft. (B) Breast MDA-MB-231 tumor xenograft. JAM-A mAb/IR700 (*Probe*) retains in tumor xenograft tissue compared with controls after tail vein injection. 48 h after injection, tumor tissue was snap-frozen followed by frozen tissue slicing, slide preparation, and fluorescent microscopy. Pseudo pink/red – IR700 fluorescence; pseudo blue – DAPI. Scale bar – 25- μ m. Quantitative analysis of IR700 intensities in prostate PC3pip tumor (C) and breast MDA-MB-231 tumor (D) xenografts after tail injection of JAM-A mAb/IR700 (*Probe*). Values represent mean of IR700 fluorescence per field of view (FOV) of the tumor xenografts during fluorescent microscopy (see A and B above). Controls: 1) mix of JAM-A mAb and JAM-A mAb/IR700 conjugates (2-to-1 ratio, respectively) – *Probe competition*; 2) non-specific mouse IgG/IR700 conjugates – *Norm Ab*, and 3) *IR700 alone*. The fluorescence of PC3pip and MDA-MB-231 xenografts was analyzed separately. Vertical bars – SD. Data were normalized to the levels of IR700 fluorescence of IR700 alone group; $n = 5$ per each group; fifteen FOV per group were analyzed by ImageJ software. * – $p < 0.0001$ to IR700 alone; † – $p < 0.001$ to Norm Ab and Probe competition (by *t*-test).

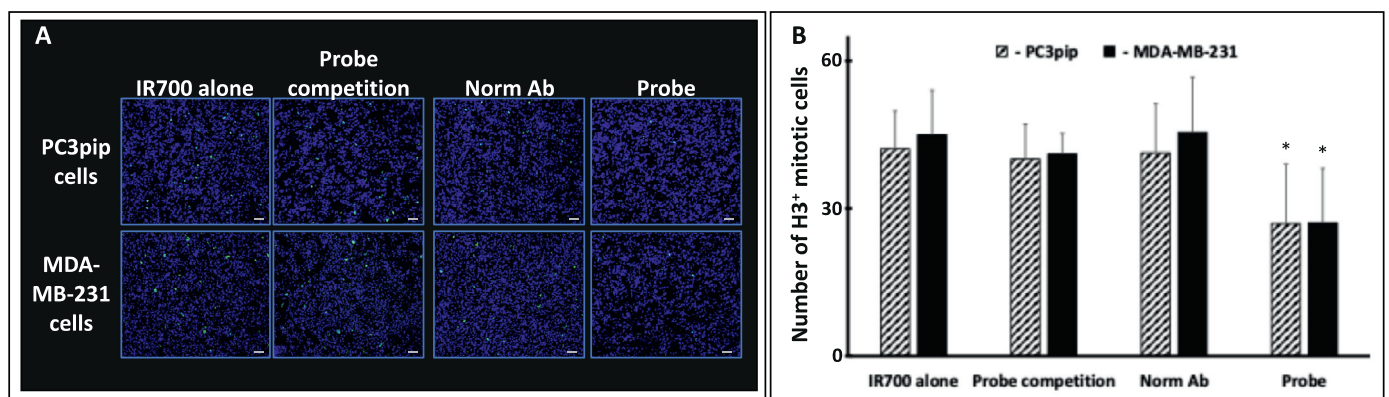


Fig. 5. JAM-A mAb/IR700 down-regulates number of mitotic cells in tumor xenograft. (A) Immunohistochemistry staining of PC3pip and MDA-MB-231 tumor xenograft tissue for phospho-histone H3⁺ (mitosis). Tissue was collected 48-h after a single JAM-A mAb/IR700 *i.v.* injection (*Probe*) and then it was snap-frozen followed by staining of 10- μ m frozen sections. Controls: 1) mix of JAM-A mAb and JAM-A mAb/IR700 conjugates (2-to-1 ratio, respectively) – *Probe competition*; 2) non-specific mouse IgG/IR700 conjugates – *Norm Ab*, and 3) *IR700 alone*. Colors: false green – H3⁺ mitotic cells, false blue – DAPI. Scale bar – 50- μ m. (B) Quantitative analysis of mitotic cells in tumor xenografts. Values represent average number of H3⁺ mitotic cells in ten fields of view at 100 \times . Vertical bars – SD; $n = 5$ per each group, * – $p < 0.05$ to controls, by ANOVA test.

in both PC3pip and MDA-MB-231 tumors 48-h after JAM-A mAb/IR700 treatment (see Fig. 5B). The highest absolute number of mitotic cells was detected in mouse spleens (see Supplementary Fig. S6A). However, the levels of H3⁺ mitotic cells in mice that were treated with JAM-A mAb/IR700 conjugates were similar to controls in tested organs (see Supplementary Fig. S6B). These observations may indicate that JAM-A mAb preserve its activity *in vivo* and once JAM-A mAb/IR700 binds to target protein it may reduce proliferation of malignant cells rather than the normal cells of the internal organs tested.

Discussion

To our knowledge, this is the first study of molecular imaging the JAM-A protein as a biomarker in human prostate and breast cancer tumors. We found that JAM-A expressing tumors may be easily visualized *in vivo*. Additionally, a single dose of JAM-A mAb was enough to significantly reduce number of mitotic cells in the prostate and breast tumors but not in mouse internal organs *in vivo*.

JAM-A was initially identified as a cell junction protein that is responsible for epithelial cell organization and tissue integrity [42,43]. JAM-A exerts these functions through the homophilic binding of JAM-A on adjacent cells, enhancement of integrin function on the same cell, and interaction with integrins on adjacent cells [44]. JAM-A-deficient mice show no major defects but do display an altered wound healing phenotype due to delayed fibroblast invasion [45]. Work over the past decade in the context of cancer has demonstrated that JAM-A regulates both pro- and anti-tumorigenic processes in a cancer-specific manner and may be useful as a biomarker of malignancy for certain cancer types [44,46]. For example, reduced adhesion resulting from JAM-A down-regulation in gastric [47], pancreatic [48], and kidney [49] cancers is associated with increased tumor cell invasion. The majority of recent studies support an intrinsic, pro-tumorigenic role for JAM-A in regulating the cell self-renewal, cancer cell proliferation, and tumor cell invasion across multiple cancer types including glioblastoma multiforme [36,50], multiple myeloma [34,51] diffuse large B-cell lymphoma [52], squamous cell carcinoma of the neck [53], cervical cancer [54], non-small cell lung cancer [55], nasopharyngeal cancer [56], with conflicting reports in gastric [57], and BCa [58–62], and with absence of reports in human PCa. Several groups successfully tied the levels of JAM-A expression in cancer tissue and patient survival [34,35,47,55,61,63].

To develop our conjugates for the current study, we used a J10.4 clone of anti-JAM-A mAb that inhibits receptor dimerization and has shown anti-proliferative effects to malignant cells that was confirmed by others [34]. So, when a strong, specific, and dose-dependent inhibition of PC3pip and MDA-MB-231 cell proliferation was also confirmed in our initial studies *in vitro*, we used this Ab to develop an optical imaging probe. Next, a substantial cytoplasmic JAM-A expression was detected in the human PCa PC3pip cell line. Further, we confirmed a distinct membrane staining for the JAM-A protein in the human BCa cells. These patterns of the JAM-A expression are in agreement with recently published data [35].

Here, we also proved that the *i.v.* injected IR700-conjugated JAM-A mAb accumulated in the prostate and breast tumor xenografts and bound to JAM-A⁺ tumor cells. We have also demonstrated here the possibility of non-invasive NIR imaging of the JAM-A⁺ cells in prostate and breast tumors *in vivo*. Indeed, JAM-A Ab/IR700-dependent fluorescence of prostate and breast tumors was 1.5–5-fold higher than IR700-fluorescent signal from tumors in mice which were treated with controls. Additionally, *ex vivo* JAM-A Ab/IR700-dependent fluorescence of excised tumors was 2.5–3-fold higher than IR700-fluorescence of controls and mainly observed at the core of both prostate and breast tumor xenografts.

In the current study liver and kidney showed the highest IR700 fluorescence both *in vivo* and *in vitro*. However, levels of NIR IR700 signal from these organs were similar in all animals treated with IR700 conjugates (see Supplementary Figs. S3B and 4B). Assum-

ing that anti-JAM-A mAb (J10.4 clone) is recommended by vendor (<https://www.scbt.com/p/jam-a-antibody-j10-4>) for detection of JAM-A protein of mouse, rat and human origin, these findings may suggest that there was a non-specific accumulation of the IR700 conjugates in liver and kidney that may be related to IgG Fc-receptor binding [64–67] rather than a distinct JAM-A mAb/IR700 uptake. Indeed, some recent *in vivo* molecular imaging studies showed that highly specific recombinant mAb directed against the human HER2 (trastuzumab) [68] and J591, a PSMA-specific mAb [69], revealed strong levels of fluorescent from the internal organs at Days 1–4 post-injection which were comparable with ones from the tumor xenografts. Altogether, it may indicate that both organs might be a temporary trap for IgG/IR700 conjugates [40].

Another possible explanation of the high TBR found in the study might be attributed to significant differences between human and murine JAM-As, leading to an artificially high TBR due to lack of binding of JAM-A mAb to murine JAM-As. In contrary to this assumption, in our parallel studies when JAM-A mAb was used to assess its activity to mouse cancer cells, we found that JAM-A mAb treatment may delay metastasis of the mouse 4T1 BCa cells to the lungs *in vivo*, indicating presence of affinity of J10.4 clone to the JAM-A of the mouse origin (Supplementary Fig. S7).

Based on published data (<https://www.proteinatlas.org/ENSG00000158769-F11R/tissue>) JAM-A protein is widely expressed with low (breast) and moderate (prostate) levels in humans that would make it somewhat difficult to discriminate between pathological and normal tissues. Nevertheless, the agent, that we tested here, demonstrated a sufficient TBR to visualize the tumors and showed similar pharmacokinetics to the highly specific humanized anti-EGFR or anti-PSMA mAbs [68,69].

JAM-A has been reported to interfere apoptosis [63,66,67,70], cell proliferation [34,55,71], cell cycle arrest at the G1/S boundary [55], cellular motility and invasiveness [34,71] of cancer cells as well as a proliferation, adhesion, and self-renewal of CD133⁺ cells but not CD133⁻ or neural progenitor cells [36]. Our *in vitro* tests showed a strong dose-dependent activity of the JAM-A mAb in both PC3pip and MDA-MB-231 proliferation assays. This substantial level of anti-proliferative activity is in agreement with published data [36]. However, it does not corroborate with a published report where prostate PC3 cancer cells did not respond to the 6F4 anti-JAM-A mAb treatment [72] that may indicate an importance of inhibition of JAM-A dimerization by direct targeting with J10.4 clone of anti-JAM-A mAb for propagation of PC3 cancer cell line [72].

One of the important aspects of this study is *in vivo* evidence of antitumor activity of the JAM-A mAb/IR700 on established models. The direct targeting with JAM-A mAb/IR700 conjugates was able to downregulate markers of proliferating activity in xenografted mice with the human tumors. *Ex vivo* analysis demonstrated the JAM-A-targeted IR700 conjugates induced *in vivo* inhibition of proliferation, as a significant decrease of phospho-histone H3 staining was observed for both PC3pip and MDA-MB-231 cancer models. Additionally, there was a delay of BCa cell metastasis *in vivo* during a short course of JAM-A mAb therapy (Supplementary Fig. S7) that positively corroborates with the most recent attempt to target multiple myeloma malignant xenograft by blocking anti-JAM-A mAb. This study demonstrated an efficacy of 20-day course of anti-JAM-A therapy that led to inhibition of progression of tumor xenografts *in vivo* with a possible downregulation of double positive multiple myeloma CD138⁺/JAM-A⁺ cells [34]. It worth to note, however, that the applicability of the current probe as a therapeutic agent is of limited by its origin and it should be humanized for any possible application in humans. Nevertheless, the current probe, as it is, might be useful for experimental animal photoimmunotherapy [73]. Indeed, additionally to anti-cancer activity of the unlabeled JAM-A mAb, the IR700 conjugates [74] may have a potential to target JAM-A^{high} expressing cancer cells after subsequent local exposure to NIR light that turns on this photochemical "death" switch, resulting in the rapid

and highly selective immunogenic cell death of targeted cancer cells [73].

Conclusion

An *in vivo* JAM-A-specific NIR-imaging of human-derived PCa and BCa xenografts is presented. JAM-A mAb/IR700 conjugates are injected and bind specifically to tumor JAM-A⁺ cells. A single injection of this agent is diminished number of mitotic cells in cancerous tissue of mice bearing heterotopic tumors. Since, JAM-A mAb/IR700 conjugates have the potential to subtract surrounding normal tissue and depict the specific accumulation of antibody within the targeted breast and prostate tumors, this agent may be adapted to local tumor targeted photodynamic therapy [73].

Declaration of Competing Interest

The authors declare that they have no known competing financial interests or personal relationships that could have appeared to influence the work reported in this paper.

CRediT authorship contribution statement

E. Walker: Conceptualization, Data curation, Formal analysis, Investigation, Methodology, Project administration, Resources, Supervision, Validation, Visualization, Writing - original draft, Writing - review & editing. **S.M. Turaga:** Data curation, Investigation. **X. Wang:** Data curation, Investigation. **R. Gopalakrishnan:** Data curation, Investigation. **S. Shukla:** Data curation, Formal analysis, Investigation. **J.P. Basilion:** Conceptualization, Formal analysis, Funding acquisition, Methodology, Resources, Supervision, Validation, Writing - review & editing. **J.D. Lathia:** Conceptualization, Formal analysis, Funding acquisition, Methodology, Resources, Supervision, Validation, Writing - review & editing.

Funding

The research leading to these results was supported by the NINDS of the NIH (R01 NS089641), the Cleveland Clinic VeloSano Bike Ride Immunology Pilot Grant, and Cleveland Clinic Innovations.

Supplementary materials

Supplementary material associated with this article can be found, in the online version, at [doi:10.1016/j.tranon.2020.101007](https://doi.org/10.1016/j.tranon.2020.101007).

References

- S.B. Giordano, W. Gradishar, Breast cancer: updates and advances in 2016, *Curr. Opin. Obstet. Gynecol.* 29 (2017) 12–17.
- B.F. Hankey, et al., Cancer surveillance series: interpreting trends in prostate cancer – part I: evidence of the effects of screening in recent prostate cancer incidence, mortality, and survival rates, *J. Natl. Cancer Inst.* 91 (1999) 1017–1024.
- R. Siegel, D. Naishadham, A. Jemal, Cancer statistics, 2012, *CA Cancer J. Clin.* 62 (2012) 10–29.
- K.B. Stitzenberg, Y.N. Wong, M.E. Nielsen, B.L. Egleston, R.G. Uzzo, Trends in radical prostatectomy: centralization, robotics, and access to urologic cancer care, *Cancer* 118 (2012) 54–62.
- G.P. Swanson, J.W. Basler, Prognostic factors for failure after prostatectomy, *J. Cancer* 2 (2011) 1–19.
- M. Han, et al., Biochemical (prostate specific antigen) recurrence probability following radical prostatectomy for clinically localized prostate cancer, *J. Urol.* 169 (2003) 517–523.
- G.R. Gibson, et al., A comparison of ink-directed and traditional whole-cavity re-excision for breast lumpectomy specimens with positive margins, *Ann. Surg. Oncol.* 8 (2001) 693–704.
- F.J. Fleming, et al., Intraoperative margin assessment and re-excision rate in breast conserving surgery, *Eur. J. Surg. Oncol.* 30 (2004) 233–237.
- E. Hollemans, et al., Prostate carcinoma grade and length but not cribriform architecture at positive surgical margins are predictive for biochemical recurrence after radical prostatectomy, *Am. J. Surg. Pathol.* 44 (2020) 191–197.
- E. Walker, et al., A protease-activated fluorescent probe allows rapid visualization of keratinocyte carcinoma during excision, *Cancer Res.* 80 (2020) 2045–2055.
- X. Wang, et al., Photodynamic therapy is an effective adjuvant therapy for image-guided surgery in prostate cancer, *Cancer Res.* 80 (2020) 156–162.
- D. van den Ouden, R. Kranse, W.C. Hop, T.H. van der Kwast, F.H. Schroder, Microvascular invasion in prostate cancer: prognostic significance in patients treated by radical prostatectomy for clinically localized carcinoma, *Urol. Int.* 60 (1998) 17–24.
- A.S. Leong, Z. Zhuang, The changing role of pathology in breast cancer diagnosis and treatment, *Pathobiology* 78 (2011) 99–114.
- G.A. Sonn, et al., Fluorescent image-guided surgery with an anti-prostate stem cell antigen (PSCA) diabody enables targeted resection of mouse prostate cancer xenografts in real time, *Clin. Cancer Res.* 22 (2016) 1403–1412.
- T. Nagaya, Y.A. Nakamura, P.L. Choyke, H. Kobayashi, Fluorescence-guided surgery, *Front. Oncol.* 7 (2017) 314.
- P.S. Low, S. Singhal, M. Srinivasarao, Fluorescence-guided surgery of cancer: applications, tools and perspectives, *Curr. Opin. Chem. Biol.* 45 (2018) 64–72.
- B. Suman, et al., Real-time fluorescence image-guided oncologic surgery, *Adv. Cancer Res.* 124 (2014) 171–211.
- M. Verdoes, K. Oresic Bender, E. Segal, W.A. van der Linden, S. Syed, N.P. Withana, L.E. Sanman, M. Bogyo, Improved quenched fluorescent probe for imaging of cysteine Cathepsin activity, *J. Am. Chem. Soc.* 135 (2013) 14726–14730.
- M. Miampamba, J. Liu, A. Harootyan, A.J. Gale, S. Baird, S.L. Chen, Q.T. Nguyen, R.Y. Tsien, J.E. González, Sensitive *in vivo* visualization of breast cancer using ratiometric protease-activatable fluorescent imaging agent, AVB-620, *Theranostics* 7 (2017) 3369–3386.
- M.J. Whitley, et al., A mouse-human phase 1 co-clinical trial of a protease-activated fluorescent probe for imaging cancer, *Sci. Transl. Med.* 8 (2016) 320ra4–320ra4.
- Y. Urano, et al., Rapid cancer detection by topically spraying a γ -glutamyltranspeptidase-activated fluorescent probe, *Sci. Transl. Med.* 3 (2011) 110ra119–110ra119.
- E.J. Ter Wee, et al., Development, preclinical safety, formulation, and stability of clinical grade bevacizumab-800CW, a new near infrared fluorescent imaging agent for first in human use, *Eur. J. Pharm. Biopharm.* 104 (2016) 226–234.
- M.L. Korb, et al., Use of monoclonal antibody-IRDye800CW bioconjugates in the resection of breast cancer, *J. Surg. Res.* 188 (2014) 119–128.
- M.S. Bradbury, et al., Clinically-translated silica nanoparticles as dual-modality cancer-targeted probes for image-guided surgery and interventions, *Integr. Biol.* 5 (2013) 74–86.
- K.A. Kelly, et al., Detection of early prostate cancer using a hepsin-targeted imaging agent, *Cancer Res.* 68 (2008) 2286–2291.
- J. Napp, et al., Time-domain *in vivo* near infrared fluorescence imaging for evaluation of matriptase as a potential target for the development of novel, inhibitor-based tumor therapies, *Int. J. Cancer* 127 (2010) 1958–1974.
- M.R. Darragh, et al., Tumor detection by imaging proteolytic activity, *Cancer Res.* 70 (2010) 1505–1512.
- M. Kawakami, T. Okaneya, K. Furihata, O. Nishizawa, T. Katsuyama, Detection of prostate cancer cells circulating in peripheral blood by reverse transcription-PCR for hKlK2, *Cancer Res.* 57 (1997) 4167–4170.
- C.A. Foss, et al., Radiolabeled small-molecule ligands for prostate-specific membrane antigen: *in vivo* imaging in experimental models of prostate cancer, *Clin. Cancer Res.* 11 (2005) 4022–4028.
- T. Yogo, K. Umezawa, M. Kamiya, R. Hino, Y. Urano, Development of an activatable fluorescent probe for prostate cancer imaging, *Bioconjug. Chem.* 28 (2017) 2069–2076.
- X. Wang, D. Ma, W.C. Olson, W.D. Heston, *In vitro* and *in vivo* responses of advanced prostate tumors to PSMA ADC, an auristatin-conjugated antibody to prostate-specific membrane antigen, *Mol. Cancer Ther.* 10 (2011) 1728–1739.
- K. Kuroda, H. Liu, S. Kim, M. Guo, V. Navarro, N.H. Bander, Saporin toxin-conjugated monoclonal antibody targeting prostate-specific membrane antigen has potent anticancer activity, *Prostate* 70 (2010) 1286–1294.
- X. Wang, et al., Photodynamic therapy is an effective adjuvant therapy for image-guided surgery in prostate cancer, *Cancer Res.* 80 (2020) 156–162.
- A.G. Solimando, et al., JAM-A as a prognostic factor and new therapeutic target in multiple myeloma, *Leukemia* 32 (2018) 736–743, [doi:10.1038/leu.2017.287](https://doi.org/10.1038/leu.2017.287).
- A.M. Rosager, et al., Expression and prognostic value of JAM-A in gliomas, *J. Neurooncol.* 135 (2017) 107–117.
- J.D. Lathia, et al., High-throughput flow cytometry screening reveals a role for junctional adhesion molecule a as a cancer stem cell maintenance factor, *Cell Rep.* 6 (2014) 117–129.
- E.A. Severson, W.Y. Lee, C.T. Capaldo, A. Nusrat, C.A. Parkos, Junctional adhesion molecule A interacts with Afadin and PDZ-GEF2 to activate Rap1A, regulate beta1 integrin levels, and enhance cell migration, *Mol. Biol. Cell* 20 (2009) 1916–1925.
- R.M. Perera, et al., Internalization, intracellular trafficking, and biodistribution of monoclonal antibody 806: a novel anti-epidermal growth factor receptor antibody, *Neoplasia* 9 (2007) 1099–1110.
- X. Wang, et al., Theranostic agents for photodynamic therapy of prostate cancer by targeting prostate-specific membrane antigen, *Mol. Cancer Ther.* 15 (2016) 1834–1844.
- J. Jin, B. Krishnamachary, Y. Mironchik, H. Kobayashi, Z.M. Bhujwalla, Phototheranostics of CD44-positive cell populations in triple negative breast cancer, *Sci. Rep.* 6 (2016) 27871, [doi:10.1038/srep27871](https://doi.org/10.1038/srep27871).
- H. Goto, et al., Identification of a novel phosphorylation site on histone H3 coupled with mitotic chromosome condensation, *J. Biol. Chem.* 274 (1999) 25543–25549.
- I. Martin-Padura, et al., Junctional adhesion molecule, a novel member of the im-

- munoglobulin superfamily that distributes at intercellular junctions and modulates monocyte transmigration, *J. Cell Biol.* 142 (1998) 117–127.
- [43] U.P. Naik, M.U. Naik, K. Eckfeld, P. Martin-DeLeon, J. Spychala, Characterization and chromosomal localization of jam-1, a platelet receptor for a stimulatory monoclonal antibody, *J. Cell Sci.* 114 (2001) 539–547.
- [44] T. Steinbacher, D. Kummer, K. Ebnet, Junctional adhesion molecule-A: functional diversity through molecular promiscuity, *Cell Mol. Life Sci.* 75 (2018) 1393–1409.
- [45] V.G. Cooke, M.U. Naik, U.P. Naik, Fibroblast growth factor-2 failed to induce angiogenesis in junctional adhesion molecule-A-deficient mice, *Arterioscler. Thromb. Vasc. Biol.* 26 (2006) 2005–2011.
- [46] C. Zhao, et al., Overexpression of junctional adhesion molecule-A and EphB2 predicts poor survival in lung adenocarcinoma patients, *Tumour Biol.* 39 (2017) 1010428317691000.
- [47] J.Y. Huang, et al., Low junctional adhesion molecule-A expression correlates with poor prognosis in gastric cancer, *J. Surg. Res.* 192 (2014) 494–502.
- [48] D. Fong, et al., Low expression of junctional adhesion molecule a is associated with metastasis and poor survival in pancreatic cancer, *Ann. Surg. Oncol.* 19 (2012) 4330–4336.
- [49] P. Gutwein, et al., Downregulation of junctional adhesion molecule-A is involved in the progression of clear cell renal cell carcinoma, *Biochem. Biophys. Res. Commun.* 380 (2009) 387–391.
- [50] A.G. Alvarado, et al., Coordination of self-renewal in glioblastoma by integration of adhesion and microrna signaling, *Neuro-Oncology* 18 (2016) 656–666.
- [51] K.R. Kelly, et al., Junctional adhesion molecule-A is overexpressed in advanced multiple myeloma and determines response to oncolytic reovirus, *Oncotarget* 6 (2015) 41275–41289.
- [52] P.P. Xu, et al., Jam-A overexpression is related to disease progression in diffuse large B-cell lymphoma and downregulated by lenalidomide, *Sci. Rep.* 7 (2016) 7433–7442.
- [53] T. Kakuki, M. Kurose, K. Takano, Dysregulation of junctional adhesion molecule-A via p63/gata-3 in head and neck squamous cell carcinoma, *Oncotarget* 7 (2016) 33887–33900.
- [54] T. Akimoto, et al., Analysis of the expression and localization of tight junction transmembrane proteins, claudin-1, -4, -7, occludin and JAM-A, in human cervical adenocarcinoma, *Histol. Histopathol.* 31 (2016) 921–931.
- [55] M. Zhang, et al., Overexpression of JAM-A in non-small cell lung cancer correlates with tumor progression, *PLoS One* 8 (2013) e79173.
- [56] Y. Tian, et al., Junctional adhesion molecule-A, an epithelial-mesenchymal transition inducer, correlates with metastasis and poor prognosis in human nasopharyngeal cancer, *Carcinogenesis* 36 (2015) 41–48.
- [57] K. Ikeo, et al., Junctional adhesion molecule-A promotes proliferation and inhibits apoptosis of gastric cancer, *Hepatogastroenterology* 62 (2015) 540–545.
- [58] K. Brennan, et al., Junctional adhesion molecule-A is co-expressed with HER2 in breast tumors and acts as a novel regulator of HER2 protein degradation and signaling, *Oncogene* 32 (2013) 2799–2804.
- [59] E.A. McSherry, K. Brennan, L. Hudson, A.D. Hill, A.M. Hopkins, Breast cancer cell migration is regulated through junctional adhesion molecule-A-mediated activation of Rap1 GTPase, *Breast Cancer Res.* 13 (2011) R31.
- [60] Y. Wang, W.Y. Lui, Transforming growth factor- β 1 attenuates junctional adhesion molecule-A and contributes to breast cancer cell invasion, *Eur. J. Cancer* 48 (2012) 3475–3487.
- [61] M. Murakami, et al., Abrogation of junctional adhesion molecule-A expression induces cell apoptosis and reduces breast cancer progression, *PLoS One* 6 (2011) e21242.
- [62] M.U. Naik, T.U. Naik, A.T. Suckow, M.K. Duncan, U.P. Naik, Attenuation of junctional adhesion molecule-A is a contributing factor for breast cancer cell invasion, *Cancer Res* 68 (2008) 2194–2220.
- [63] E.A. McSherry, et al., JAM-A expression positively correlates with poor prognosis in breast cancer patients, *Int. J. Cancer* 125 (2009) 1343–1351.
- [64] H. Shen, et al., Expression of Fc fragment receptors of immunoglobulin G (Fc gammaRs) in rat hepatic stellate cells, *Dig. Dis. Sci.* 50 (2005) 181–187.
- [65] A. Suwanichkul, S.E. Wenderfer, Differential expression of functional Fc-receptors and additional immune complex receptors on mouse kidney cells, *Mol. Immunol.* 56 (2013) 369–379.
- [66] C.L. Anderson, L.P. Ganesan, J.M. Robinson, The biology of the classical Fc γ receptors in non-hematopoietic cells, *Immunol. Rev.* 268 (2015) 236–240.
- [67] H.H. Radeke, I. Janssen-Graalfs, E.N. Sowa, Opposite regulation of type II and III receptors for immunoglobulin G in mouse glomerular mesangial cells and in the induction of anti-glomerular basement membrane (GBM) nephritis, *J. Biol. Chem.* 277 (2002) 27535–27544.
- [68] K. Sano, M. Mitsunaga, T. Nakajima, P.L. Choyke, H. Kobayashi, In vivo breast cancer characterization imaging using two monoclonal antibodies activatably labeled with near infrared fluorophores, *Breast Cancer Res.* 14 (2012) R61.
- [69] T. Nakajima, et al., Targeted, activatable, in vivo fluorescence imaging of prostate-specific membrane antigen (PSMA) positive tumors using the quenched humanized J591 antibody-iodocyanine green (ICG) conjugate, *Bioconjug. Chem.* 22 (2011) 1700–1705.
- [70] P. Danthi, M.W. Hansberger, J.A. Campbell, J.C. Forrest, T.S. Dermody, JAM-A-independent, antibody-mediated uptake of reovirus into cells leads to apoptosis, *J. Virol.* 80 (2006) 1261–1270.
- [71] K. Magara, et al., Elevated expression of JAM-A promotes neoplastic properties of lung adenocarcinoma, *Cancer Sci.* 108 (2017) 2306–2314.
- [72] L. Goetsch, et al., A novel role for junctional adhesion molecule-A in tumor proliferation: modulation by an anti-JAM-A monoclonal antibody, *Int. J. Cancer* 132 (2013) 1463–1474.
- [73] H. Kobayashi, P.L. Choyke, Near-infrared photoimmunotherapy of cancer, *Acc. Chem. Res.* 52 (2019) 2332–2339, doi:10.1021/acs.accounts.9b00273.
- [74] M. Mitsunaga, M. Ogawa, N. Kosaka, LT Rosenblum, PL Choyke, H. Kobayashi, Cancer cell-selective in vivo near infrared photoimmunotherapy targeting specific membrane molecules, *Nat. Med.* 17 (2011) 1685–1691, doi:10.1038/nm.2554.